

# QUANTIFYING BLOOD FLOW DIVISION AT BIFURCATIONS FROM ROTATIONAL ANGIOGRAPHY

I. Waechter<sup>1</sup>, J. Bredno<sup>2</sup>, R. Hermans<sup>3</sup>, D.C. Barratt<sup>1</sup>, J. Weese<sup>2</sup>, D.J. Hawkes<sup>1</sup>

<sup>1</sup> Centre for Medical Image Computing, University College London, United Kingdom,

<sup>2</sup> Philips Research Europe, Aachen, Germany

<sup>3</sup> Philips Medical Systems, X-ray Pre-Development, Best, the Netherlands

## ABSTRACT

For assessment of cerebrovascular diseases, it is beneficial to obtain information about the hemodynamics of the vessel system. Recently, we presented a method to quantify blood flow in a single blood vessel segment from rotational angiography. In this paper, we extend the method to bifurcations. A model-based method is proposed which estimates the mean flow, the waveform and the flow division at the bifurcation. The method is validated on experimental data using a phantom for a healthy and a stenosed carotid bifurcation. The average error for the estimate of the flow division was 8%.

**Index Terms**— Flow quantification, rotational angiography, bifurcation, flow modeling

## 1. INTRODUCTION

For diagnosis, treatment planning and outcome control of cerebrovascular diseases, such as atherosclerosis, aneurysms, or arteriovenous malformations (AVM), it is beneficial to obtain three-dimensional (3D) information on vessel morphology and hemodynamics.

Rotational angiography now is routinely used to determine information about the 3D geometry. To achieve this, contrast agent is injected and x-ray images are acquired while the c-arm rotates around the head of the patient. Recently, we presented a model-based method to quantify blood flow in a single blood vessel segment from rotational angiography [1]. In this method, we optimize parameters of the model against the observed development of the contrast agent concentration in order to deduce mean volume flow and the flow waveform over the cardiac cycle. In this paper, we extend the method to bifurcations. The additional parameter of interest is the flow division at the bifurcation. The flow division states which fraction of the volumetric flow in the mother branch is going into which daughter branch.

The flow division at a bifurcation is of clinical interest for the evaluation of a stenosis at one branch or for the evaluation of an arteriovenous malformation (AVM). Both lead to changes of the resistances which then lead to a change in the flow division at the bifurcation.

Several different approaches for the determination of blood flow information from planar angiography have been reported previously. However, these methods are either not suitable to determine quantitative flow estimates or they work only on single segments of blood vessels.

Methods based on the estimation of the bolus arrival time (BAT) using time intensity curves (TICs) at different points in the vessel tree, can work on multiple segments [2]. However, they assume that the flow is constant in time. This neglects the very important characteristic of blood flow that it is pulsatile. It was shown that BAT methods cannot give reliable results in the case of pulsatile flow and it is also not possible to determine the blood flow waveform [3].

Methods based on distance intensity curves (DICs) can determine a blood flow waveform [4], but they assume that flow is constant in space. Therefore, they can only be applied to one segment at a time and this segment is not allowed to taper significantly [3]. If the method should be applied to more than one segment, it could be applied for each segment separately. However, the further the observation is away from the injection, the more difficult it is to apply the method due to the dispersion of the bolus.

For the extraction of flow from rotational angiography, only two approaches have been reported to date. Chen et al. [5] use a BAT method. Therefore, the problems described above apply. Appaji and Noble [6] use an optical flow method to reconstruct flow from rotational angiography, but they have not reported any quantitative results yet and only consider one segment.

We propose a model-based method to estimate the mean flow, the waveform and the flow division at the bifurcation from rotational angiography. Knowledge about the conservation of flow is used to support the flow quantification in segments which are further away from the injection site.

## 2. METHODS

### 2.1. Preparation for flow quantification

To prepare the flow quantification, our method determines a flow map and a reliability map from the rotational angio-

graphic image sequence (see Fig. 1). To initialize this, the user has to indicate the start point of the mother branch and the end points of the two daughter branches of the bifurcation. The user can also divide a branch into segments if the radius varies significantly in one branch and he can mark segments as unreliable. Then, the 3D centerline, given by the points  $P^i(l)$  and the 3D radii  $R^i(l)$ , where  $l$  is the length along the segment, are extracted for each branch  $i = 1, 2, 3$  as described by Waechter et al. [7]. After that, the flow map and the reliability can be extracted.

The flow map is represented by an image, where the intensity is the mean attenuation due to the contrast agent, the horizontal dimension is time  $t$  and the vertical dimension is length  $l$  along the centerline of the vessel. The extracted flow map is given by

$$\mathbf{F}_E^i(l, t) = \frac{I(\Pi(P^i(l), G(t)), t)}{\mathbf{L}^i(l, t)}. \quad (1)$$

where  $I(x, t)$  is the rotational angiographic image sequence,  $\Pi(P(l), G(t))$  is the projection function,  $G(t)$  gives the geometric parameters of the rotation.  $\mathbf{L}^i(l, t)$  gives the length of the vessel segment along the x-ray beam; it is determined using the centerline, the radii and the geometric parameters of the rotation.

The reliability map gives the reliability of each entry of the flow map. Due to the rotation, two errors can occur in the flow map: errors due to foreshortening and errors due to overlapping vessels [8]. For example, the second branch of the bifurcation can overlap with the first branch in some frames. The reliability map is defined as

$$\mathbf{R}_F^i(l, t) = \begin{cases} 0 & , \text{if vessel overlap is detected} \\ 0 & , \text{if indicated by the user} \\ \cos \theta & , \text{otherwise,} \end{cases} \quad (2)$$

where vessel overlap is defined as the case when more than one vessel segment intersects with the x-ray beam and  $\theta$  is the angle between the x-ray beam and the vessel centerline, which gives the degree of foreshortening. The reliability map is determine automatically from the centerline and radii. An example for the flow maps and the corresponding reliability maps of a bifurcation is given in Fig. 1(d) and 1(e). Each flow map and reliability map corresponds to one branch. The visible pattern in the flow map is introduced by the pulsatile flow.

## 2.2. Flow model

For the flow quantification, a flow model, based on the physics of blood flow and contrast agent transport, is used. The flow model includes a model of the injection and a model of the waveform. The flow model is used to simulate a flow map given certain flow parameters.

The blood flow waveform in the mother branch is given by

$$Q_B(t) = \bar{Q}_B \cdot p_\alpha(t), \quad (3)$$

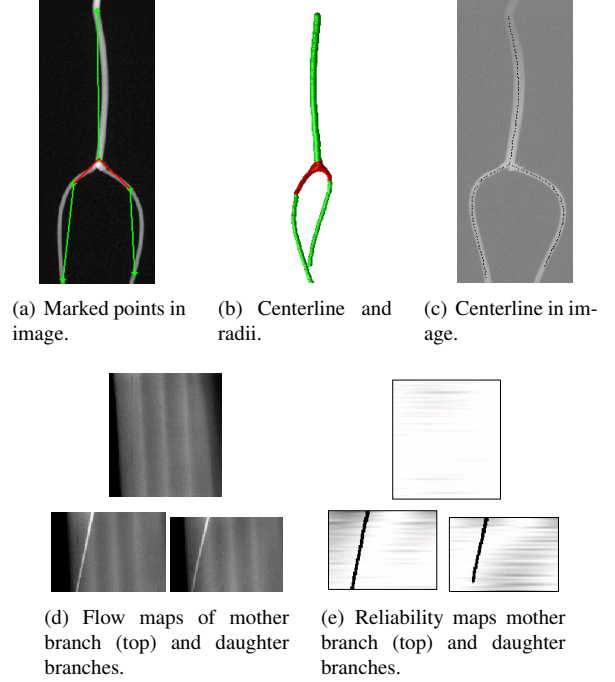


**Fig. 1.** Extraction of flow map and reliability map.

where  $\bar{Q}_B$  is the mean volumetric flow rate and  $p_\alpha(t)$  is a parametric description of the waveform [1]. The total flow  $Q_T$  in the mother branch ( $i = 1$ ) is given by

$$Q_T^1(t) = Q_B(t) + m \cdot Q_I(t), \quad (4)$$

where  $Q_I(t)$  is the flow of the injection and  $m$  is a mixing factor. If we assume that the vessel walls are rigid, then the flows in the daughter branches ( $i = 2, i = 3$ ) can be described by

$$Q_T^2(t) = \beta \cdot Q_T^1(t) \quad (5)$$

$$Q_T^3(t) = (1 - \beta) \cdot Q_T^1(t) \quad (6)$$

where  $\beta$  denotes the flow division. For each segment  $j$  of branch  $i$  with nodes  $S_j$  and with radii  $R^i$ , the effective radius is determined by

$$R_{\text{eff}}^j = \left( \sum_{k \in S_j} \frac{1}{(R^i(l_k))^2} \right)^{-0.5}. \quad (7)$$

The flow is assumed to be axially symmetric and laminar. The vessel is divided into  $N$  laminae and the radius in the middle of lamina  $n$  is given by

$$r_n^j = \frac{n - 0.5}{N} R_{\text{eff}}^j, n \in [1, 2, \dots, N]. \quad (8)$$

The velocity in lamina  $n$  of segment  $j$  in branch  $i$  is then given by

$$v^{i,j}(n, t) = \frac{Q_T^i(t)}{2\pi \sum_{n=1}^N p(r_n^j) r_n^j} \cdot p(r_n^j), \quad (9)$$

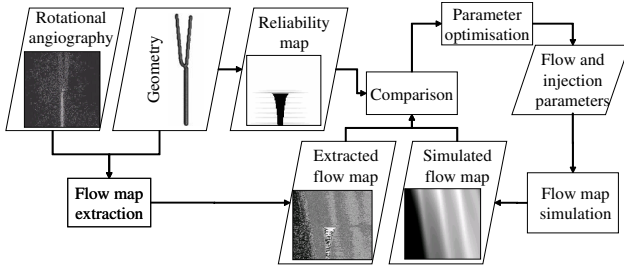


**Fig. 2.** Overview of the flow map fitting algorithm.

where  $p(r)$  describes the flow profile across the cross section.

The concentration of iodine, which is the attenuating component of the contrast agent, at the injection site is determined by

$$C^1(n, 0, t) = c \cdot \frac{Q_I(t)}{Q_T^1(t)}, n \in [1, 2, \dots, N] \quad (10)$$

where  $c$  is the concentration of iodine in the contrast agent. The transport of contrast agent is based on a model of convection and diffusion. The convection is implemented as described by Rhode et al. [4] and the diffusion is implemented as a low pass filter. The result of this simulation is the temporal and spatial development of the contrast agent for each branch  $C^i(r, l, t)$ . Finally, the simulated flow map  $\mathbf{F}_S^i$  for each branch is given by

$$\mathbf{F}_S^i(l, t) = \frac{1}{N} \sum_{n=1}^N C^i(n, l, t). \quad (11)$$

### 2.3. Flow map fitting

For the flow quantification, the simulated flow maps  $\mathbf{F}_S$  are fitted to the extracted flow map  $\mathbf{F}_E$ . During the fitting, the error given by

$$E(\mathbf{F}_S) = \sum_{l=1}^L \sum_{t=1}^T [\mu E_1(l, t)^2 + \nu E_2(l, t)^2] \cdot \mathbf{R}_F(l, t), \quad (12)$$

where

$$E_1(l, t) = f \cdot \mathbf{F}_S(l, t) - \mathbf{F}_E(l, t)$$

$$E_2(l, t) = f \cdot \nabla \mathbf{F}_S(l, t) - \nabla \mathbf{F}_E(l, t)$$

is minimized and optimal values for the model parameters are determined, in particular, the mean flow  $\bar{Q}_B$ , the waveform  $p_\alpha(t)$ , and the flow division  $\beta$ .  $f$  is the attenuation calibration factor which is determined during the fitting process.  $\mu$  and  $\nu$  are weighting factors. An overview of the flow map fitting algorithm is given in Fig. 2.

### 2.4. Validation setup

The validation is based on images from an experimental setup, which consists of a pulsatile flow circuit, a clinical

contrast agent injector (MarkVProVis, Medrad) and a rotational x-ray system (Allura Xper with an FD20 detector, Philips Medical Systems). Rotational image sequences were acquired following a contrast agent injection (Ultravist-370, Schering) into one of the bifurcation phantoms. The phantom was placed in an elliptical, water filled cylinder to generate realistic noise, beam hardening, and scatter. The ground truth flow was measured by an electromagnetic flow meter (EMF).

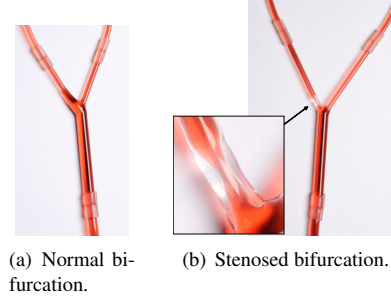


**Fig. 3.** Phantoms for carotid bifurcations.

The first phantom is a bifurcation which consists of three simple tubes; the second represents a normal carotid bifurcation with a carotid bulb, where the base of the internal carotid artery characteristically widens immediately after the bifurcation; the third represents a carotid bifurcation with a stenosis. Images of the second two bifurcation phantoms are shown in Fig. 3.

	Value	Unit
<b>Acquisition</b>		
Frame rate	30	[1/sec]
Rotation speed	55	[°/sec]
Rotation range	205	[°]
Number images	120	[]
Duration	4	[sec]
<b>Injection</b>		
Max flow	[180, 360]	[ml/min]
Duration	2, 3	[sec]
<b>Flow</b>		
Mean flow	300	[ml/min]
Pulsatility	0.5, 0.7, 0.8, 0.9	[]
Flow division at bifurcation	0.5, 0.67, 0.83	[]

**Table 1.** Table with parameters of experiments

Parameters of the acquisition, injection and flow are given in Table 1. The flow division at the bifurcation was varied by varying the upstream resistance at one branch of the bifurcation. Overall 28 datasets were acquired.

For each dataset, the flow map and reliability map were determined. Then, the mean flow, the flow waveform and the flow division factor were determined using the flow map fitting. For each, the mean absolute percentage error was deter-

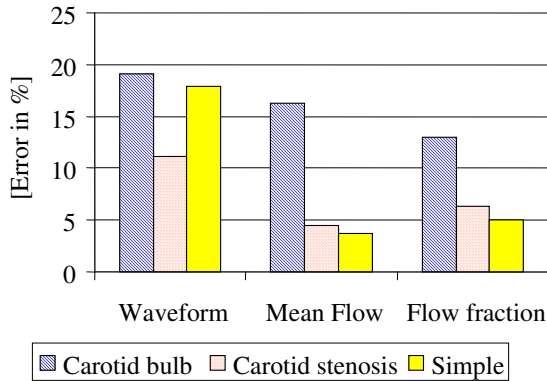


Fig. 4. Errors of flow estimates from flow map fitting.

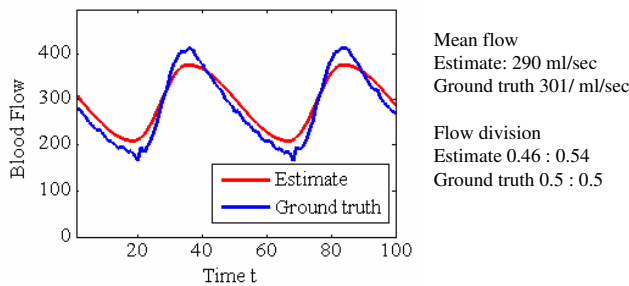


Fig. 5. Flow parameters estimated using the flow map fitting.

mined.

### 3. RESULTS

The overall error in the mean flow was 8.5%; the overall error in the waveform was 15.1%; the overall error in the flow division was 8.5%. The results for the different phantoms are detailed in Fig. 4. An example of the estimated flow parameters is shown in Fig. 5 together with the ground truth.

### 4. DISCUSSION AND CONCLUSION

In this paper, we have presented a model based method to quantify blood flow at a bifurcation. We estimate the blood flow waveform, the mean flow, and the flow division at the bifurcation.

The model we used is very simple compared to current computational fluid dynamics models of a bifurcation. We have chosen to use this simple model because it has to be applied iteratively in the fitting procedure.

For the validation, experiments with a phantom with a carotid bulb and a phantom with a stenosis were conducted. The error of the estimate of the flow division was found to be larger for the phantom with the carotid bulb. We believe that

this is due to a secondary flow in this region. The stenosis did not present a problem for our method. This represents a significant advance on existing methods for quantifying blood flow from angiographic images which are mostly unable to handle a stenosis.

The reason why our method can handle bifurcations and changes of the radius is that it includes a model of the geometry and a model of the flow. It uses both to simulate the flow for the corresponding geometry.

### 5. REFERENCES

- [1] I. Waechter, J. Bredno, J. Weese, D. C. Barratt, and D. J. Hawkes, "Quantification of blood flow from rotational angiography," in *Medical Image Computing and Computer-Assisted Intervention (MICCAI)*, 2007.
- [2] H. Schmitt, M. Grass, R. Suurmond, T. Koehler, V. Rasche, S. Haehnel, and S. Heiland, "Reconstruction of blood propagation in three-dimensional rotational X-ray angiography (3D-RA)," *Comput. Med. Imaging. Graph.*, Sep 2005.
- [3] S. D. Shpilfoysel, R. A. Close, D. J. Valentino, and G. R. Duckwiler, "X-ray videodensitometric methods for blood flow and velocity measurement: A critical review of literature," *Med. Phys.*, vol. 27, no. 9, pp. 2008–2023, Sep 2000.
- [4] K. S. Rhode, T. Lambrou, D. J. Hawkes, and A. M. Seifalian, "Novel approaches to the measurement of arterial blood flow from dynamic digital X-ray images," *IEEE Trans. Med. Imaging*, vol. 24, no. 4, pp. 500–513, Apr 2005.
- [5] Z. Chen, R. Ning, D. Conover, and X. Lu, "Blood flow measurement by cone-beam CT bolus imaging," in *Medical Imaging, Proceedings of the SPIE*, 2006.
- [6] A. A. Appaji and J. A. Noble, "Estimating cerebral blood flow from a rotational angiographic system," in *Biomedical Imaging: Macro to Nano*, 6-9 April 2006, pp. 161–164.
- [7] I. Waechter, J. Bredno, J. Weese, and D. J. Hawkes, "Using flow information to support 3D vessel reconstruction from rotational angiography," *Medical Physics*, vol. 33, pp. 1983, 2006.
- [8] S. Y. J. Chen, J. D. Carroll, and J. C. Messenger, "Quantitative analysis of reconstructed 3-D coronary arterial tree and intracoronary devices," *IEEE Transactions on Image Processing*, vol. 21, no. 7, pp. 724–740, Jul 2002.